Adsorption Equilibrium and Desorption Activation Energy of Water Vapor on Activated Carbon Modified by an Oxidation and Reduction Treatment

Xin Li,[†,‡] Xiao Chen,[†] and Zhong Li*[,†]

The Guangdong Provincial Laboratory of Green Chemical Technology, School of Chemistry and Chemical Engineering, South China University of Technology, Guangzhou, China, 510640, and Institute of Biomaterial, College of Science, South China Agricultural University, Guangzhou, China, 510642

Activated carbon (AC) was modified by oxidation with nitric acid and microwave-assisted reduction. The textural properties and surface oxygen content as well as the surface acidities of the ACs studied were determined by nitrogen adsorption, X-ray photoelectron spectrometry, and Boehm titration. The adsorption isotherms of the water vapor were measured, and temperature-programmed desorption experiments were conducted to estimate the desorption activation energy, E_d, of water on the ACs. The results indicated that the oxidation increased the value of E_d and the adsorption capacity of water on AC in low relative humidity (RH) but decreased the adsorption capacity of water in high RH. The reduction decreased the value of E_d and the adsorption capacity of water on AC over the whole RH range. The modification of AC first by the oxidation treatment of nitric acid and then by microwave-assisted reduction treatment not only increased the adsorption capacity of water in a high RH but also greatly decreased the value of E_d. The microwave-assisted reduction of virgin or oxidized AC with hydrogen should yield a lower E_d and higher adsorption capacity of water in high RH than the reduction of that with nitrogen.

Introduction

Relative humidity (RH) is the most important factor influencing the industrial production, the preservation of goods, and human health. Too high a humidity will make house dust mites increase, allow fungi to grow on damp surfaces, and destruct the human body's hot and humid balance. Generally, in an attempt to control the RH of our environment, air-conditioning equipment has been used; however, this method has the associated problem of high energy consumption.[1] Therefore, the use of desiccants has been a good alternative for air dehumidification systems. Commonly used desiccant materials include activated carbon (AC),[2,3] activated alumina,[2,4] silica gel,[1,5,6] molecular sieves,[5,7] mesoporous materials,[8] lithium chloride,[9] calcium chloride,[9,10] and so forth. In comparison with zeolite regeneration, which requires temperatures greater than 623 K, the regeneration of water-saturated AC is relatively simple since it can be fully regenerated by only heating at 413 K.[7,11] It is well-known that the technology of dehumidification by adsorption usually consists of adsorption and desorption processes, with the amount of energy consumed in the regeneration process being considered the sole factor contributing toward the cost of dehumidification.

In addition, although ACs have a higher affinity for volatile organic compounds (VOCs) than water vapor, the presence of water vapor can severely handicap the VOC sorption capacity and change the kinetics of sorption processes, especially at high RH.[12−14]

It is also well-known that microwave-assisted reduction modification can remove a large number of water affinity groups on the surface of AC in a short time.[15,16] However, studies about how to decrease the amount of energy consumed in the regeneration process of ACs and weaken the mutual actions between water and ACs through microwave-assisted reduction modification are still scarce.

Our previous papers[17] concluded that the surface acidities of the ACs were in direct proportion to their surface oxygen contents, and the value of the desorption activation energy for water on the ACs increased with increasing surface oxygen content and decreasing pore size of the ACs. The present study attempts to reduce the amount of energy consumed in the regeneration process of ACs by the microwave-assisted reduction modification and further investigates the effects of the modification on adsorption capacity and desorption activation energy of water vapor. Temperature-programmed desorption (TPD) was used to measure the desorption activation energy of water, and X-ray photoelectron spectrometry (XPS) and the Boehm titration method were used to measure the surface oxygen content and surface properties of the ACs. The effects of pore structure and surface properties of the reduction samples on their adsorption properties and desorption activation energy of water are discussed.

TPD Theory and Model

TPD is a surface analysis technique.[18] It is usually used to estimate the binding energy between the adsorbate and the adsorbent and the activation energy of desorption.[17,19,20] These, in turn, can be used to evaluate the adsorbents and to estimate adsorption isotherms.[20]

The TPD spectrum is a plot of the rate of desorption of the adsorbate as a function of the sample temperature.[17−20] If we assume that the kinetics of the desorption process follow first-order kinetics, then we can write:

* Corresponding author. Fax: +86-20-87110608. E-mail address: cezhli@scut.edu.cn.
[†] South China University of Technology.
[‡] South China Agricultural University.

10.1021/je100024r
Published on Web 06/10/2010

$$\frac{r_d}{N_s} = -\frac{d\theta_A}{dt} = k_d\theta_A \quad (1)$$

where r_d is the desorption rate of component A from a unit mass of adsorbent (mol·min^{-1}), N_s is the maximum concentration of component A on the unit surface of the adsorbent (mol·cm^{-2}), θ_A is the transient coverage of component A, t is the time (min), and k_d is the desorption rate constant (min^{-1}), which is defined as:

$$k_d = k_0 \exp\left(-\frac{E_d}{RT}\right) \quad (2)$$

where k_0 is the pre-exponential factor (min^{-1}), E_d is the activation energy of desorption (kJ·mol^{-1}), and R is the gas constant. Substituting eq 2 into eq 1 gives:

$$\frac{r_d}{N_s} = -\frac{d\theta_A}{dt} = k_0\theta_A \exp\left(-\frac{E_d}{RT}\right) \quad (3)$$

Let us assume that the TPD experiment has been designed so that the temperature, T/K, varies with time:

$$T = T_0 + \beta_H t \quad (4)$$

where β_H is the rate of heating rate (K·min^{-1}). The time derivative of eq 3 can be expressed as:

$$\frac{1}{N_s}\frac{dr_d}{dt} = k_0\left(\frac{d\theta}{dt}\right)\exp\left(-\frac{E_d}{RT}\right) + k_0\theta_p\left(\frac{E_d}{R}\right)\frac{1}{T^2}\exp\left(-\frac{E_d}{RT}\right)\left(\frac{dT}{dt}\right) \quad (5)$$

As seen generally in the TPD curve, the maximum in the desorption rate will occur at $dr_d/dt = 0$ at which the corresponding temperature is called the peak temperature, T_p. Substituting $T = T_p$ and $dr_d/dt = 0$, eqs 2 and 3, into eq 5 leads to:

$$\ln\left(\frac{RT_p^2}{\beta_H}\right) = \frac{E_d}{R}\left(\frac{1}{T_p}\right) + \ln\left(\frac{E_d}{k_0}\right) \quad (6)$$

The corresponding TPD curves and T_p values may be obtained if a series of TPD experiments are conducted at different heating rates. A plot of $\ln(RT_p^2/\beta_H)$ versus $1/T_p$ should yield a straight line of slope E_d/R and intercept $\ln(E_d/k_0)$. Hence, the values of E_d and k_0 may be obtained from the slope and intercept, respectively.

Experimental Section

AC and Reagents. The ACs used in this study were purchased from the Liaoning Chaoyang AC Co., Ltd. (P. R. China). The sizes of the particles in these samples ranged from (20 to 40) mesh. Prior to use, they were all dried for 4 h in a vacuum at 413 K. The ACs were first subjected to 1 mol·L^{-1} HCl treatment for 24 h. After being filtered and washed, the samples were treated by 1 mol·L^{-1} NaOH for 24 h. After this treatment, the samples were washed in supersonic fields for 2 h. Then the samples were oven-dried overnight at 413 K, and the dry samples were then stored in hermetically sealed flasks until use. Such virgin samples are referred to as AC.

Prior to the oxidation of ACs, they were dried for 4 h at 413 K. A 10 g AC sample was immersed and kept in the 50 mL 13.2 mol·L^{-1} nitric acid solutions for 24 h.[21,22] Then the samples were taken out of the solution and laid in a 413 K oven for 4 h after rinsing with water. At last, the dry ACs were placed in a vacuum desiccator for use. The oxidation samples will be referred as OAC in the text.

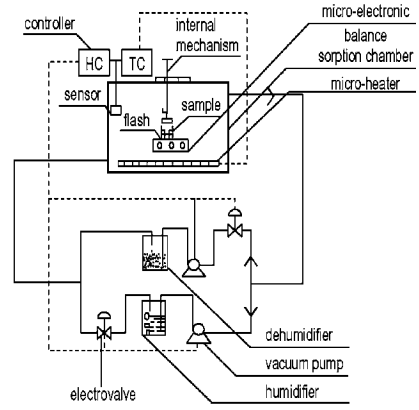

Figure 1. Experimental setup for measuring the water vapor adsorption equilibrium on the various ACs studied.

To prepare the reduced ACs, 10 g of the AC was placed in a quartz tube within a microwave chemical reactor. Then the samples were treated in hydrogen or nitrogen with a flow rate of 200 mL·min^{-1} by microwave-assisted reduction modification at 600 W for 60 min. The modified samples of AC will be referred to as RAC(H_2) and RAC(N_2) in this paper. Similarly, 10 g of the OAC were placed in a quartz tube within a microwave chemical reactor. Then the samples were treated in hydrogen or nitrogen with a flow rate of 200 mL·min^{-1} by microwave-assisted reduction modification at 600 W for 60 min. The modified samples of OAC will be referred to as ROAC(H_2) or ROAC(N_2) in this paper.

Nitrogen Adsorption Experiments. The specific surface area, pore volume, and average pore diameter of samples were measured by nitrogen adsorption at the liquid nitrogen temperature of 77 K with the help of a Micromeritics gas adsorption analyzer ASAP 2010 machine. The AC sample was degassed at 573 K for 3 h in a vacuum before the nitrogen adsorption measurements. The Brunauer−Emmett−Teller (BET) surface area was calculated from the adsorption isotherms using the standard BET equation. The pore size distributions (PSD) were determined using density functional theory (DFT) based on statistical mechanics. The average pore diameter $D_P = 4V_P/S_{BET}$ (assuming a cylindrical shape of pores) was calculated from the BET surface area and pore volume.

Determination of Isotherm of the Water Vapor on the ACs. Adsorption equilibrium experiments were performed at atmospheric pressure using the experimental setup shown in Figure 1.[17,19] This apparatus consisted of an adiabatic sorption chamber and a system for controlling the temperature and the humidity. A microelectronic balance with an accuracy of 0.0001 g was located within the adsorption chamber whose temperature and humidity could be adjusted and maintained at a constant value via the gas cycle employed. The RH was controlled to a precision of ± 3 % through the use of a dehumidifier and humidifier, while the temperature could be controlled to an accuracy of ± 0.5 K.

Experiments were conducted by first introducing 0.2 g of a sample of fresh AC into an airtight flask fitted with a cover, and the flask was then placed on the electronic microbalance located within the sorption chamber. Second, after the temperature and RH within the sorption chamber had been adjusted to a predetermined value via the temperature and humidity controllers, the flask was opened using an internal mechanism thereby allowing the adsorption of water vapor onto the ACs to commence. The weight of the sample increased gradually as the adsorption proceeded up to an equilibrium position which

Table 1. Surface Areas and Pore Structure of Modified ACs

adsorbents	S_{BET} / $m^2 \cdot g^{-1}$	V_{total} / $cm^3 \cdot g^{-1}$	$d_{average}$ / nm
AC	1071	0.6915	2.54
OAC	926.3	0.5963	2.574
RAC(N_2)	1033	0.6418	2.491
RAC(H_2)	1023	0.6338	2.479
ROAC(N_2)	1163	0.7311	2.550
ROAC(H_2)	1203	0.7686	2.556

Table 2. Elemental Analyses of Modified ACs by XPS

	atomic concentration			
adsorbents	C	N	O	Si
AC	93.28	0.1529	6.086	0.48
OAC	90.05	1.09	8.49	0.38
RAC(N_2)	95.91	0.2025	3.615	0.2734
RAC(H_2)	96.40	0.2116	3.219	0.15
ROAC(N_2)	96.34	0.4801	2.871	0.31
ROAC(H_2)	98.37	0.35	1.06	0.18

was judged to correspond to the situation when the weight of the sample hardly varied with time. At this point, the sample of AC was considered to have been saturated with water vapor, and hence the equilibrium amount adsorbed of the water vapor on a unit mass of the AC corresponding to a given RH could be obtained. A series of adsorption equilibrium experiments under different RH conditions could thereby be obtained, allowing a plot of the equilibrium amounts of water vapor adsorbed on a unit mass of AC to be plotted against the corresponding RH and hence generate the water vapor isotherm on the AC concerned.

Boehm Titration. The Boehm titration method was used to determine the number of oxygenated surface groups.[17,23] One gram of carbon sample was placed in 50 mL of the following 0.05 $mol \cdot L^{-1}$ solutions: hydrochloric acid, sodium hydroxide, sodium carbonate, and sodium bicarbonate. The vials were sealed and stirred for 24 h and filtered. Then 5 mL of each filtrate was titrated with HCl and NaOH depending on the original titrant. The numbers of acidic sites of various types were calculated using the assumption that NaOH neutralizes carboxylic, phenolic, and lactonic groups; Na_2CO_3 neutralizes carboxylic and lactonic, and $NaHCO_3$ neutralizes only carboxylic groups. The number of basic sites was calculated from the amount of HCl that reacted with the carbon.

XPS Experiments. The X-ray photoelectron spectra of the AC sample were obtained with a model PHI5600 X-ray photoelectron spectrometer. Al Kα was used for excitation, and the base pressure in the analysis chamber was $3 \cdot 10^{-9}$ mbar. For surface analysis, the specimens were fixed to the specimen holder with double-sided adhesive tape. The C1s peak of carbon with a 285.0 eV binding energy was used as a reference for correction of specimen charging. The content of carbon, oxygen, nitrogen, and silica was determined by XPS.

TPD Experiments. The TPD experiments[17,19,20] were conducted at different heating rates within the range from (5 to 8) $K \cdot min^{-1}$. In each experiment, the sample that had adsorbed the water vapor was packed into a stainless steel reaction tube (i.d., 0.3 cm; packed length, 0.5 cm). This stainless steel tube was subsequently placed in a reaction furnace and heated while a flow of N_2 gas was passed through it at a constant rate of 46.9 $mL \cdot min^{-1}$. The desorbed water vapor emerging from the outlet of the stainless steel tube was detected using a GC-9501 chromatograph fitted with a thermal conductivity detector (TCD). The effluent curves thus recorded are referred to below as TPD curves. The application of eq 6 to the experimental TPD curves allowed the activation energy for the desorption of water from the four kinds of ACs to be estimated.

Results and Discussion

Effect of the Modification on Textural Properties. Table 1 summarizes the specific surface area, the total pore volume, and average pore diameter of AC and the other five carbons after different treatments. The data in Table 1 show that the treatments greatly affect both the specific surface area and the total pore volume of the ACs studied. The liquid-phase oxidation by HNO_3 decreased the S_{BET} of the original AC sample from (1071 to 926.3) $m^2 \cdot g^{-1}$ and pore volume from (0.6915 to 0.5963) $cm^3 \cdot g^{-1}$. This indicated that the surface oxidation of the AC leads to a decrease in micropores when introducing oxygen functionality, and the thinner pore walls were more easily destroyed by the oxidizing agent. These observations are in agreement with reported results.[21,22] The treatment of the AC with H_2 or N_2 in the microwave field of 600 W for 1 h slightly decreased the S_{BET} from (1071 to 1023 or 1033) $m^2 \cdot g^{-1}$ and pore volume from (0.6915 to 0.6338 or 0.6418) $cm^3 \cdot g^{-1}$. This suggests partial surface destruction due to higher temperatures of the AC in the microwave field.[15,16]

From Table 1 it is noticed that the reduction of OAC with hydrogen or nitrogen could significantly increase S_{BET}, pore volume, and average pore diameter of the AC. This is due to the fact that more groups containing oxygen have been introduced into the carbon surface during the oxidation process; then, more surface groups can be removed from OAC than from AC by microwave heating in the reduction process, which results in the increase of S_{BET}, pore volume, and average pore diameter of the AC.[15,16] It is also observed that the specific surface areas, pore volume, and average pore diameter of the oxidized AC after the reduction with hydrogen were larger than those after the reduction with nitrogen. This suggests that hydrogen may be more suitable for the microwave reduction modification of AC because hydrogen will easily react with the groups containing oxygen on the surface of AC and form water vapor molecules at high temperature.

Surface Elemental Analyses of AC. The elemental analyses of AC were performed using XPS. In Table 2 the results of elemental analyses are shown to check whether the oxygen groups have been introduced to the carbon or removed from the carbon. A content of 1.09 % of nitrogen and 8.49 % of oxygen was detected for OAC, while only 0.35 % of nitrogen and 1.06 % of oxygen were detected for ROAC(H_2). It is clear that the oxidation can raise the amount of oxygen and nitrogen, while the reduction can decrease the amount of oxygen. The results demonstrate that oxygen functional groups could be introduced through oxidation by nitric acid and removed through the reduction by hydrogen and nitrogen in the microwave field.[15,16,21,22] It is also noticed that the oxygen content of ROAC(H_2) was much lower than that of ROAC(N_2), and the oxygen content of RAC(H_2) was much lower than that of RAC(N_2). That is to say, the reduction of virgin or oxidized

Table 3. Surface Groups of Modified ACs

	acidities ($mmol \cdot g^{-1}$)			basicity	acidic	total
adsorbents	carboxylic	lactonic	phenolic	$mmol \cdot g^{-1}$	$mmol \cdot g^{-1}$	$mmol \cdot g^{-1}$
AC	0.152	0.095	0.136	0.435	0.383	0.818
OAC	0.995	0.638	0.483	0.10	2.116	2.216
RAC(N_2)	0.108	0.083	0.085	0.479	0.276	0.755
RAC(H_2)	0.103	0.078	0.073	0.495	0.254	0.749
ROAC(N_2)	0.093	0.068	0.064	0.515	0.225	0.74
ROAC(H_2)	0.069	0.050	0.047	0.535	0.166	0.701

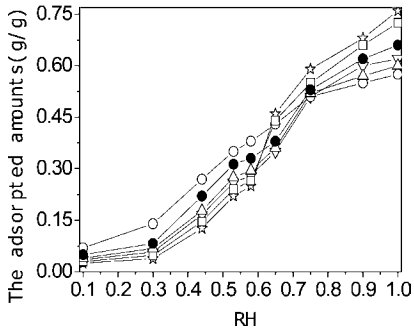

Figure 2. Adsorption isotherms of the water vapor on modified ACs at 303 K: ☆, ROAC(H_2); □, ROAC(N_2); ●, AC; ▽, RAC(H_2); △, RAC(N_2); ○, OAC.

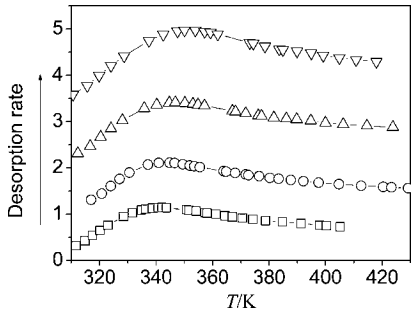

Figure 3. TPD spectrum of water on the AC at different heating rates: ▽, $\beta_H = 8$ K·min^{-1}; △, $\beta_H = 7$ K·min^{-1}; ○, $\beta_H = 6$ K·min^{-1}; □, $\beta_H = 5$ K·min^{-1}.

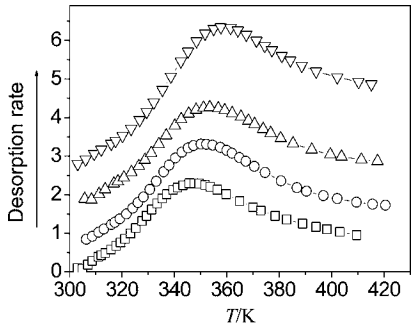

Figure 4. TPD spectrum of water on the OAC at different heating rates: ▽, $\beta_H = 8$ K·min^{-1}; △, $\beta_H = 7$ K·min^{-1}; ○, $\beta_H = 6$ K·min^{-1}; □, $\beta_H = 5$ K·min^{-1}.

AC with hydrogen should yield a smaller surface oxygen content than the reduction of that with nitrogen, in the microwave field. This showed that hydrogen was more suitable for the reduction modification of AC.

Surface Acid−Base Properties of AC. The amount of acidic surface functional groups (carboxylic, lactonic, and phenolic hydroxyl groups) is determined by the Boehm titration method. Table 3 shows the results of six kinds of ACs. It is clear that surface oxidation introduced a significant number of acid groups and significantly decreased the number of basic groups on the surface of OAC. But the surface reduction treatment results in a slight increase in the number of basic groups and significantly decreases the number of acidic groups, suggesting the removal of some oxygen groups from carbon surface due to the higher temperatures of AC in the microwave field. It is also noticed that the reduction of virgin or oxidized AC with hydrogen should yield smaller amounts of surface acid groups than the reduction with nitrogen, in the microwave field.

Effect of the Modification on Adsorption Properties of Water. Adsorption isotherms of the water vapor on different ACs at 303 K are shown in Figure 2. The shapes of all of these

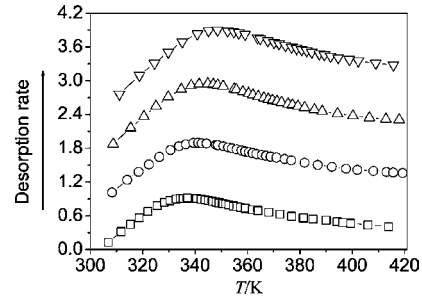

Figure 5. TPD spectrum of water on the RAC(N_2) at different heating rates: ▽, $\beta_H = 8$ K·min^{-1}; △, $\beta_H = 7$ K·min^{-1}; ○, $\beta_H = 6$ K·min^{-1}; □, $\beta_H = 5$ K·min^{-1}.

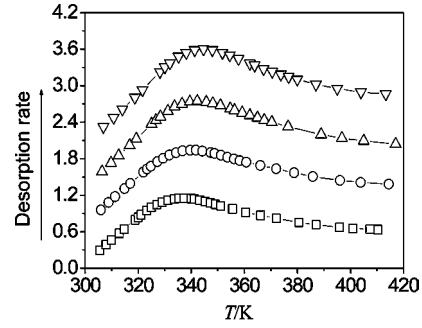

Figure 6. TPD spectrum of water on the RAC(H_2) at different heating rates: ▽, $\beta_H = 8$ K·min^{-1}; △, $\beta_H = 7$ K·min^{-1}; ○, $\beta_H = 6$ K·min^{-1}; □, $\beta_H = 5$ K·min^{-1}.

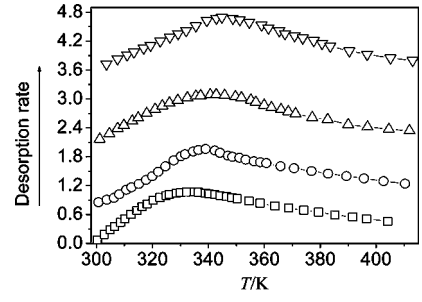

Figure 7. TPD spectrum of water on the ROAC(N_2) at different heating rates: ▽, $\beta_H = 8$ K·min^{-1}; △, $\beta_H = 7$ K·min^{-1}; ○, $\beta_H = 6$ K·min^{-1}; □, $\beta_H = 5$ K·min^{-1}.

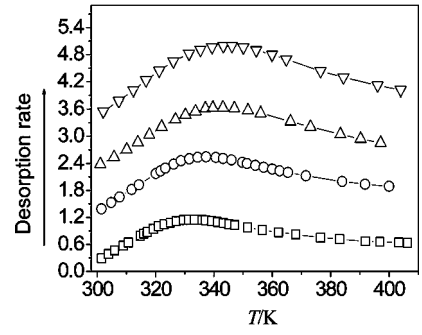

Figure 8. TPD spectrum of water on the ROAC(H_2) at different heating rates: ▽, $\beta_H = 8$ K·min^{-1}; △, $\beta_H = 7$ K·min^{-1}; ○, $\beta_H = 6$ K·min^{-1}; □, $\beta_H = 5$ K·min^{-1}.

isotherms indicate that adsorption was unfavorable in each case. It can also be seen from Figure 2 that the amounts of adsorbed water on the ROAC(H_2) and the ROAC(N_2) are higher than that on the AC in high RH and that the amount of adsorbed water on the ROAC(H_2) is the largest. But the amounts of adsorbed water on the RAC(H_2), RAC(N_2), and OAC are lower than that on the AC. This order is in agreement with the order of pore volume. This indicates that the larger the pore volume

Table 4. Desorption Peak Temperatures of Water at Different Heating Rates and Desorption Activation Energies of Water on the Modified ACs

AC	desorption peak temperature T_p/K at below heating rate				desorption activation energy, E_d	
	5 K·min^{-1}	6 K·min^{-1}	7 K·min^{-1}	8 K·min^{-1}	kJ·mol^{-1}	adj. R^2
OAC	347.2	350.0	353.2	355.6	50.78	0.9951
AC	341.7	346.0	349.4	352.7	37.22	0.9994
RAC(N_2)	336.9	341.1	345.1	348.5	33.92	0.9988
RAC(H_2)	336.7	341.1	345.1	348.2	33.58	0.9992
ROAC(N_2)	336.1	340.93	344.31	348.07	32.97	0.9963
ROAC(H_2)	333.7	339.0	343.1	346.9	28.60	0.9988

of a given AC is, the larger the amount of adsorbed water vapor is at higher RH such as that approaching 100 %. This may be ascribed to the pore-filling mechanism involved where the amount of adsorbed water was mainly dependent on the total pore volume of the AC.[11,17] Of the six ACs studied in this work, ROAC(H_2) has the largest pore volume, while OAC had the smallest. However, it is also noticed that the amounts of adsorbed water on modified ACs in low RH are in direct proportion to their total surface group contents which is different from the adsorption by the H-bonds between water and the oxygenated groups on the surface at lower RH.[17,19]

Effect of the Modification on Desorption Activation Energy of Water. Figures 3 to 8 illustrate the TPD water desorption spectra from the six kinds of the ACs at different heating rates. An obvious peak appears in each TPD spectrum due to the desorption of water vapor from the respective AC. A gradual increase in the heating rate β_H led to an increase in the peak temperature T_p. The values of all of the peak temperatures can be obtained from the TPD spectra depicted in Figures 3 to 8 and which are listed in Table 4.

Knowing the values of T_p for the different heating rates employed, it is possible to estimate the desorption activation energy of water from the various ACs through the use of eq 6. The desorption activation energy for the various ACs studied are listed in Table 4 from which it is seen that the values for ACs OAC, AC, RAC(N_2), RAC(H_2), ROAC(N_2), and ROAC(H_2) were 50.78 kJ·mol^{-1}, 37.22 kJ·mol^{-1}, 33.92 kJ·mol^{-1}, 33.58 kJ·mol^{-1}, 32.97 kJ·mol^{-1}, and 28.60 kJ·mol^{-1}, respectively. Thus, the desorption activation energy for water from OAC had the greatest value, and that from ROAC(H_2) was the smallest. Although the average pore diameter of the micropores in OAC was the largest, the desorption activation energy of water from OAC (or ROAC(H_2)) was obviously the greatest (or smallest) because the amount of surface acid groups and oxygen content on OAC (or ROAC(H_2)) was greater (or smaller) than that on other five carbons. The higher concentration of surface acid groups and oxygen content increased the interaction between the water molecules and the surface and thus increased the magnitude of the activation energy required for water desorption. The amounts of surface acid groups and oxygen content on the surfaces of RAC(N_2), RAC(H_2), and ROAC(N_2) were almost the same, as indicated by the data listed in Tables 2 and 3; therefore, the desorption activation energy of water on them was close. This was due to the amounts of surface acid groups and oxygen content being the main factor influencing the desorption activation energy of water when their average micropore diameters are similar, as shown by the data in Table 1.

Conclusions

To decrease the amount of energy consumed in the regeneration process, it should be practical to reduce the surface acidities or surface oxygen contents of the ACs by the microwave-assisted reduction modification. TPD was successfully applied to readily obtain a desorption activation energy of water vapor on different ACs. The parameter of the desorption activation energy can reflect the interactions between water and ACs. In summarizing the results, the following conclusions may be drawn:

(1) The oxidation increased the value of E_d and the adsorption capacity of water on AC in low RH but decreased the adsorption capacity of water in high RH. The reduction decreased the value of E_d and the adsorption capacity of water on AC over the whole RH range. The desorption activation energy of water vapor on the OAC was 50.78 kJ·mol^{-1}; however, the desorption activation energy of water on the ROAC(H_2) was only 28.60 kJ·mol^{-1}.

(2) Microwave-assisted reduction was an effective method to modify the surface properties of AC and reduced the value of desorption activation energy of water. In the microwave field, the reduction of AC or OAC with hydrogen should yield a smaller value of E_d and the adsorption capacity of water in high RH than the reduction of that with nitrogen.

(3) The desorption activation energy of water decreased with a decrease of surface acid groups and oxygen content on AC when their average micropore diameters were almost equal. The amounts of adsorbed water on the modified ACs in low RH were in direct proportion to their total surface group contents, and the adsorption performance of water on the modified ACs at high RH mainly depends on their total pore volume.

Literature Cited

(1) Ohashi, F.; Maeda, M.; Inukai, K.; Suzuki, M.; Tomura, S. Study on intelligent humidity control materials: Water vapor adsorption properties of mesostructured silica derived from amorphous fumed silica. *J. Mater. Sci.* **1999**, *34*, 1341–1346.

(2) Kim, J. H.; Lee, C. H.; Kim, W. S.; Lee, J. S.; Kim, J. T.; Suh, J. K.; Lee, J. M. Adsorption equilibria of water vapor on alumina, zeolite 13X, and a zeolite X/activated carbon composite. *J. Chem. Eng. Data* **2003**, *48*, 137–141.

(3) Kim, M. B.; Ryu, Y. K.; Lee, C. H. Adsorption equilibria of water vapor on activated carbon and DAY zeolite. *J. Chem. Eng. Data* **2005**, *50*, 951–955.

(4) Serbezov, A. Adsorption equilibrium of water vapor on F-200 activated alumina. *J. Chem. Eng. Data* **2003**, *48*, 421–425.

(5) Wang, Y.; Levan, M. D. Adsorption Equilibrium of Carbon Dioxide and Water Vapor on Zeolites 5A and 13X and Silica Gel: Pure Components. *J. Chem. Eng. Data* **2009**, *54*, 2839–2844.

(6) Chung, T. W.; Chung, C. C. Increase in the amount of adsorption on modified silica gel by using neutron flux irradiation. *Chem. Eng. Sci.* **1998**, *53*, 2967–2972.

(7) Tashiro, Y.; Kubo, M.; Katsumi, Y.; Meguro, T.; Komeya, K. Assessment of adsorption-desorption characteristics of adsorbents for adsorptive desiccant cooling system. *J. Mater. Sci.* **2004**, *39*, 1315–1319.

(8) Oh, J. S.; Shim, W. G.; Lee, J. W.; Kim, J. H.; Moon, H.; Seo, G. Adsorption equilibrium of water vapor on mesoporous materials. *J. Chem. Eng. Data* **2003**, *48*, 1458–1462.

(9) Li, X. W.; Zhang, X. S.; Wang, G.; Cao, R. Q. Research on ratio selection of a mixed liquid desiccant: Mixed LiCl-$CaCl_2$ solution. *Solar Energy* **2008**, *82*, 1161–1171.

(10) Aristov, Y. I.; Glaznev, I. S.; Freni, A.; Restuccia, G. Kinetics of water sorption on SWS-1L (calcium chloride confined to mesoporous silica

gel): Influence of grain size and temperature. *Chem. Eng. Sci.* **2006**, *61*, 1453–1458.
(11) Yang, R. T. *Adsorbents: fundamentals and applications*; John Wiley and Sons: New York, 2003.
(12) Kaplan, D.; Nir, I.; Shmueli, L. Effects of high relative humidity on the dynamic adsorption of dimethyl methylphosphonate (DMMP) on activated carbon. *Carbon* **2006**, *44*, 3247–3254.
(13) Li, J.; Li, Z.; Liu, B.; Xia, Q. B.; Xi, H. X. Effect of Relative Humidity on Adsorption of Formaldehyde on Modified Activated Carbons. *Chin. J. Chem. Eng.* **2008**, *16*, 871–875.
(14) Rodriguez-Mirasol, J.; Bedia, J.; Cordero, T.; Rodriguez, J. J. Influence of water vapor on the adsorption of VOCs on lignin-based activated carbons. *Sep. Sci. Technol.* **2005**, *40*, 3113–3135.
(15) Carrott, P. J. M.; Nabais, J. M. V.; Ribeiro Carrott, M. M. L.; Menendez, J. A. Thermal treatments of activated carbon fibres using a microwave furnace. *Microporous Mesoporous Mater.* **2001**, *47*, 243–252.
(16) Valente Nabais, J. M.; Carrott, P. J. M.; Ribeiro Carrott, M. M. L.; Menéndez, J. A. Preparation and modification of activated carbon fibres by microwave heating. *Carbon* **2004**, *42*, 1315–1320.
(17) Li, X.; Li, Z.; Xia, Q. B.; Xi, H. X.; Zhao, Z. X. Effects of textural properties and surface oxygen content of activated carbons on the desorption activation energy of water. *Adsorpt. Sci. Technol.* **2006**, *24*, 363–374.
(18) Rudzinski, W.; Borowiecki, T.; Panczyk, T.; Dominko, A. On the applicability of Arrhenius plot methods to determine surface energetic heterogeneity of adsorbents and catalysts surfaces from experimental TPD spectra. *Adv. Colloid Interface Sci.* **2000**, *84*, 1–26.
(19) Li, X.; Li, Z.; Xia, Q. B.; Xi, H. X. Effects of pore sizes of porous silica gels on desorption activation energy of water vapour. *Appl. Therm. Eng.* **2007**, *27*, 869–876.
(20) Park, J. H.; Yang, R. T. Predicting adsorption isotherms of low-volatile compounds by temperature programmed desorption: Iodine on carbon. *Langmuir* **2005**, *21*, 5055–5060.
(21) Moreno-Castilla, C.; Lopez-Ramon, M. V.; Carrasco-Marin, F. Changes in surface chemistry of activated carbons by wet oxidation. *Carbon* **2000**, *38*, 1995–2001.
(22) El-Hendawy, A. N. A. Influence of HNO_3 oxidation on the structure and adsorptive properties of corncob-based activated carbon. *Carbon* **2003**, *41*, 713–722.
(23) Jorge, M.; Schumacher, C.; Seaton, N. A. Simulation study of the effect of the chemical heterogeneity of activated carbon on water adsorption. *Langmuir* **2002**, *18*, 9296–9306.

Received for review January 9, 2010. Accepted May 30, 2010. The work is supported by the National Natural Science Foundation of China (Grant No. 20936001 and No. 20906034) and the Science & Technology Foundation of Guangdong Province.

JE100024R